Conformational Toggle Switches Implicated in Basal Constitutive and Agonist-Induced Activated States of 5-Hydroxytryptamine-4 Receptors

Lucie P. Pellissier, Jessica Sallander, Mercedes Campillo, Florence Gaven, Emilie Queffeulou, Marion Pillot, Aline Dumuis, Sylvie Claeysen, Joël Bockaert, Leonardo Pardo

Conformational toggle switches implicated in basal constitutive and agonist-induced activated states of 5-HT_4 receptors

Lucie Pellissier[1], Jessica Sallander[1], Mercedes Campillo, Florence Gaven, Emilie Queffeulou, Marion Pillot, Aline Dumuis, Sylvie Claeysen, Joël Bockaert and Leonardo Pardo

CNRS UMR 5203, Institut de Génomique Fonctionnelle, Montpellier, F-34094, France ; INSERM, U661, Montpellier, F-34094, France ; Universités Montpellier 1, 2, Montpellier, F-34094, France (L.Pe., F.G., E.Q., M.P., A.D., S.C., J.B.);

Laboratori de Medicina Computacional, Unitat de Bioestadística, Facultat de Medicina, Universitat Autònoma de Barcelona, 08193 Bellaterra, Spain (J.S., M.C., L.Pa.).

Running title: 5-HT_4R agonists act differently on a double toggle switch

Corresponding author:

Joël Bockaert

Institut de Génomique Fonctionnelle

141 Rue de la Cardonille

34094 Montpellier Cedex 5

France,

Tel: +33 467 14 29 30

Fax: +33 467 54 24 32

E-mail: joel.bockaert@igf.cnrs.fr

Manuscript information:

Number of text pages: 24

Number of tables: 1

Number of figures: 6

Number of references: 37

Number of words in the *Abstract:* 250

Introduction: 638

Discussion: 1110

Abbreviations:

5-HT, 5-hydroxytryptamine; GPCRs, G protein-coupled receptors; TM, transmembrane; β_2-AR, β_2-adrenergic receptor.

ABSTRACT

The extended classical ternary complex model predicts that a GPCR exists in only two inter-convertible states: an inactive R and an active R*. However, different structural active R* complexes may exist in addition to a silent inactive Rg (R ground state). Here we demonstrate, in a cellular context, that several R*s of 5-HT_4 receptors involve different side chain conformational toggle switches. Using site-directed mutagenesis and molecular modelling approaches, we show that the basal constitutive receptor (R*basal) results from stabilization of an obligatory double toggle switch (T3.36 from inactive *g*- to active *g*+ and W6.48 from inactive *g*+ to active *t*). Mutation of either T or W to A resulted in a lowering of the activity of the R*basal similar to the Rg. The T3.36A mutation shows that the T3.36 toggle switch plays a minor role in the stabilization of R* induced by 5-HT (R*-5-HT) and BIMU8 (R*-BIMU8), and is fully required in the stabilization of R* induced by S-zacopride, cisapride, and RS 67333 (R*-benzamides). Thus, benzamides stabilize R*-benzamides by forming a specific hydrogen bond with T3.36 in the active *g*+ conformation. Conversely, R*-BIMU8 was likely the result of a direct conformational transition of W6.48 from inactive *g*+ to active *t* by hydrogen bonding of this residue to a carboxyl group of BIMU8. Surprisingly, the W6.48 toggle switch was not necessary for receptor activation by the natural agonist 5-HT. R*-5-HT is probably attained through other routes of activation. Thus, different conformational arrangements occur during stabilization of R*basal, R*-5-HT, R*-benzamides and R*-BIMU8.

INTRODUCTION

G-protein-coupled receptors (GPCRs) are allosteric molecules in equilibrium with many different conformational states (Bond et al., 1995; Samama et al., 1993). GPCRs adopt at least one inactive (R) and several active (R*) states (Alves et al., 2003; Baneres et al., 2005; Ghanouni et al., 2001; Okada et al., 2001; Swaminath et al., 2004). R* states can be reached, even in the absence of agonists or mutations (called here basal constitutively active R* or R*basal), whereas chemically different ligands can stabilize different R*s. Partial agonists may stabilize a specific receptor state different from the R* of full agonist. For example, using circular dichroism difference spectra of the purified 5-HT_4 receptor, we have previously found that free (or neutral antagonist-occupied), agonist-occupied (partial or full agonist) and silent (inverse agonist-occupied) receptors involved different arrangement of the e_2 loop (Baneres et al., 2005). Inactive R state of family A GPCRs is generally not the equivalent to the "silent" state of the cis-retinal-rhodopsin receptor complex called the ground state (Rg) (Palczewski et al., 2000; Park et al., 2008). Recent insights into the β_2-adrenergic receptor (β_2-AR) structure indicate that, even in the presence of the partial inverse agonist carazolol, this receptor is certainly not under the Rg state and adopts a structural feature of the R*s (a relatively open "ionic lock") (Cherezov et al., 2007; Rosenbaum et al., 2007). Therefore, the Rg state may only be reached with full inverse agonists such as the cis-retinal and the R state may be, in some receptors, already a R* (Palczewski et al., 2000).

One of the main questions in GPCR molecular pharmacology is to understand the structural arrangements of the 7 transmembrane (TM) helices that occur to stabilize either Rg or the different R*s. Notably, some main arrangement and rearrangement events during activation seem to be common, at least in family A GPCRs (Kobilka, 2007; Ruprecht et al., 2004; Schertler, 2005; Smit et al., 2007).

The recent crystal structure of the ligand-free opsin, which contains several features characteristic of R*s (Park et al., 2008), has shown that the intracellular part of TM6 is tilted outwards by 6-7 Å, while TM5 moves towards TM6 by 2-3 Å. In addition, conformational changes occurring to generate either Rg or R* states are accomplished by rearrangement of side chains forming different networks of

interactions between helices (Rosenbaum et al., 2007; Shi et al., 2002; Smit et al., 2007). The structure of metarhodopsin I by electron crystallography (Ruprecht et al., 2004; Schertler, 2005), experimental studies of rhodopsin (Lin and Sakmar, 1996), as well as computer simulations associated with mutagenesis of β_2-adrenergic (Shi et al., 2002), 5-HT_{2A} (Visiers et al., 2002), CB1 (McAllister et al., 2004) and histamine H_1 receptors (Jongejan et al., 2005) have shown that W6.48 of the conserved CWxPFF motif of TM6 undergoes a conformational transition, from pointing toward TM7 in the inactive state, to pointing toward TM5 in the agonist-induced R* (Ruprecht et al., 2004; Schertler, 2005). The side chain at position 3.36 has also been suggested to act as a rotamer toggle switch simultaneously with W6.48 in the histamine H_1 and cannabinoid (CB1) receptors (Jongejan et al., 2005; McAllister et al., 2004).

In this study, we have investigated the 5-HT_4 receptor (5-HT_4R), and its ability to stabilize different R*s. The focus was mainly put on the roles of the W6.48 rotamer toggle switch and its associated toggle switch at position 3.36. We found that both toggle switches were required for stabilizing the basal R* state (called R*basal), none of them were fully implicated in stabilizing the R* reached in the presence of 5-HT (called R*-5-HT), whereas the T3.36 and the W6.48 toggle switches were implicated in stabilizing the R* in the presence of synthetic agonists belonging to either the benzamide or aryl ketone classes (called R*-benzamides), or to a benzimidazolone class (called R*-BIMU 8).

MATERIALS AND METHODS

Plasmid construct

HA-tagged-5-HT_4 receptor cDNAs in pRK5 were generated by fusing the sequence of the HA epitope (YPYDVPDYA) to a cleavable signal peptide (MVLLLILSVLLLKEDVRGSAQS) derived from the metabotropic glutamate receptor 5 (mGlu5R). This sequence was inserted into the pRK5 vector using Xba I and BsrG I restriction sites. Then, full-length mouse 5-$HT_{4(a)}$R cDNAs were subcloned in frame using BsrG I and Hind III. HA-5-HT_4-T3.36A, HA-5-HT_4-T3.36S, HA-5-HT_4-T3.36C, HA-5-HT_4-W6.48A receptor mutants were generated from HA-5-$HT_{4(a)}$R, cloned in pRK5, with the Quick Change Site-Directed Mutagenesis Kit (Stratagene, Amsterdam, Netherlands).

Membrane preparation and radioligand binding assay

Membranes were prepared from transiently transfected cells plated on 15-cm dishes and grown in DMEM with 10% dialyzed foetal calf serum (dFCS) as described in Claeysen *et al.* (Claeysen et al., 2003). The membrane solubilized in 50 mM HEPES (pH 7.4; 5 mg of protein in 1 ml of solution) were stored at -80°C until use. Membrane suspension (about 10 µg), diluted in 100 µl of 50 mM HEPES containing 10 mM pargyline and 0.01% ascorbic acid, was incubated at 20°C for 30 min with 100 µl [^{3}H]GR 113808 (specific activity: 82 Ci/mmole) and 50 µl of buffer or competing drugs. For saturation analysis assays, various concentration of [^{3}H]GR 113808 (0.001-0.8 nM) were used. BIMU8 (10 µM) was used to determine non-specific binding. Protein concentration was determined by using the bicinchoninic acidic method.

Cell surface ELISA

COS-7 cells were transfected with HA-tagged-5-HT_4R, WT or mutants cDNAs. Cells were grown on 96-well plates in DMEM medium with 10% dFCS and fixed as described previously (Barthet et al., 2005). Cells were then incubated with anti-HA antibody at 0.6 µg/ml for 60 min in the same buffer and incubated with anti-rabbit/HRP conjugate (Amersham Pharmacia Biotech) at 1 µg/ml for 60 min.

Chromogenic substrate was added (Supersignal® ELISA femto-maximum sensitivity (Pierce, Perbio-Brebières, France). Chemiluminescence was detected and quantified by a Wallac Victor^2 luminescence counter.

Determination of cAMP production in transfected cells

COS-7 cells were transfected with the appropriate cDNA and seeded into 24-well plates (100 000 cells/well). 24 hours post-transfection, a 10 min-stimulation with the appropriate concentrations of drugs was performed as previously described (Barthet et al., 2005). Quantification of cAMP production was performed by Homogenous Time Resolved Fluorescence (htrf®) using the cAMP Dynamic kit (Cisbio International, Bagnols-sur-Cèze, France), according to the manufacturer's instructions.

Data analysis

The dose-response curves were fitted using GraphPad Prism and the following equation for monophasic dose-response curves: $y = (y_{max} - y_{min}) / 1 + [(x / EC_{50}) n_H] + y_{min}$, where EC_{50} is the concentration of the compound necessary to obtain 50% of the maximal effect and n_H is the Hill coefficient. Competition and saturation experiments were analysed by non-linear regression using GraphPad Prism as previously described (Ansanay et al., 1996). All data represented correspond to the mean ± SEM of three independent experiments performed in triplicate. Statistical analysis was carried out with the t test using GraphPad Prism 3.0 software.

Nomenclature of side chain conformation

The side chain conformation has been categorized into *gauche*- (*g*-: $0° < \chi_1 < 120°$), *trans* (*t*: $120° < \chi_1 < 240°$), or *gauche*+ (*g*+: $240° < \chi_1 < 360°$) depending on the value of the torsional χ_1 angle.

Numbering scheme of GPCRs

Residues are identified by the generic numbering scheme of Ballesteros & Weinstein (Ballesteros and Weinstein, 1995) that allows easy comparison among residues in the 7TM segments of different receptors.

Computational model of the ligand-receptor complexes

A model of the 5-HT_4R was constructed by homology modelling using the crystal structure of the β_2-adrenergic receptor (PDB code 2RH1) (Cherezov et al., 2007; Rosenbaum et al., 2007) as template. The 5-HT, BIMU8, and S-zacopride, ligands were docked, by interactive computer graphics, into the receptor model with their protonated side chain interacting with D3.32 in TM3 (Shi and Javitch, 2002). The Duan *et al.* (2003) force field (Duan et al., 2003) was used for peptides and the general Amber force field (GAFF) (Wang et al., 2004) and HF/6-31G*-derived RESP atomic charges were used for the ligands. Molecular dynamics simulations, in a explicit lipidic bilayer, of the ligand-receptor complexes were performed with the Sander module of AMBER 9 (Case et al., 2006) using the protocol previously described (Jongejan et al., 2005).

Drugs

The following compounds were used: BIMU8 N-[(1R,5S)-8-methyl-8-azabicyclo[3.2.1]oct-3-yl]-2,3-dihydro-3-iso-propyl-2-oxo-1H-benzimidazol-1-carboxamide hydrochloride, S-zacopride (*S*)-*N*-(1-azabicyclo[2.2.2]oct-3-yl)-4-amino-5-chloro-2-methoxybenzamide monohydrochloride, Cisapride *cis*-4-amino-5-chloro-N-{1-[3-(4-fluoro-phenoxy)propyl]-3-methoxy-4-piperidinyl}-2-methoxy benzamide, RS 67333 1-(4-amino-5-chloro-2-methoxy-phenyl)-3-(1-butyl-4-piperidinyl)-1-propanone, RO116-1148 2,3-dihydrobenzo-(1,4)-dioxine-5-carboxylic acid 1-butylpiperidin-4-ylmethylamide hydrochloride

RESULTS

*The role of T3.36 and W6.48 in stabilizing the basal constitutive activity of 5-HT$_4$ receptors (R*basal).*

We have previously shown that the constitutive activity of the histamine H_1 receptor was dependent on the nature of the residue at position 3.36 (Jongejan et al., 2005). When serine, present in the WT H_1 receptor was substituted by threonine or cysteine, the basal constitutive activity increased dramatically, occluding the histamine activation; whereas the constitutive activity was inexistent when serine was substituted by alanine. In biogenic amine receptors, the 3.36 position is rarely occupied by threonine (1%) and more often by cysteine (56%) or serine (31%). Interestingly, position 3.36 is occupied by threonine in 5-HT$_4$Rs. This may explain why 5-HT$_4$Rs have such a high constitutive activity. We engineered the T3.36A/S/C mutant receptors to study the role of the short and polar side chain of T3.36 in the constitutive activity of the 5-HT$_4$R. By using different plasmid concentrations, we managed to obtain similar cell surface expression of the WT 5-HT$_4$R and T3.36A/S/C mutants. This was confirmed by using an Elisa assay (Fig. 1A) but also by Scatchard analysis using the specific labelled 5-HT$_4$R ligand [^{3}H]GR 113808, as described previously (Claeysen et al., 1999) (see Fig. 1A and its legend). The T3.36A mutation almost abolished the constitutive activity (Fig. 1B), indicating that the hydrogen bond capability of T3.36 plays an important role in stabilizing R* adopted by constitutively active 5-HT$_4$Rs. T3.36S/C mutations provide a way of identifying the conformation of T3.36 in the active state of the R*basal because of the different side chain rotamer distribution of threonine from those of serine or cysteine, when located in an α-helical structure (Fig. 1C) (Ballesteros et al., 2000). The conformations of the short and β-branched side chain of threonine are limited to the *g*+ (85% of the side chains) and *g*- (15%) because the *t* conformation is unfavourable due to the steric clash of the side chain methyl group with the backbone carbonyl at the i-3 position (McGregor et al., 1987). In contrast, serine can adopt either the *g*+ (52%), *g*- (20%) or *t* (28%) rotamer conformation. The fact that T3.36S reduces the constitutive activity of the receptor to a level close to the value observed in the T3.36A mutation precludes the serine-specific *t* conformation as the active conformation. Cysteine is restricted to the *g*+ (71%) or *t* (29%) conformation because of the

steric clash between the Sγ atom and the carbonyl oxygen of residue i-3 in the *g*- conformation (McGregor et al., 1987). The unchanged constitutive activity of the T3.36C mutation, relative to WT, points to the common *g*+ conformation of cysteine and threonine as the active conformation, in agreement with previous proposals (Jongejan et al., 2005). We, thus, propose that T3.36 in the 5-HT_4R undergoes a conformational transition from the inactive *g*- to the active (R*basal) *g*+ conformation. Modecular modelling showed that this conformational transition is only feasible if the side chain of W6.48 modifies its conformation simultaneously, in a concerted manner, from the inactive *g*+ to the active *t* conformation (Fig. 1D). Both the W6.48 and the T3.36 concerted toggle switches were absolutely necessary to adopt the R* constitutive active state (R*basal). Indeed, as previously described, the W6.48A mutant (Joubert et al., 2002) as well as the T3.36A mutant were under the Rg state (Fig. 1B).

In order to be certain that both mutations (T3.36A and W6.48A) were stabilizing the 5-HT_4R under a Rg state, we studied the activities of these mutants as a function of the receptor density. As seen in Fig. 2A the basal activity of the WT receptor increased proportionally to the plasmid concentration and up to 31 pmol/mg whereas the basal activity of both T3.36A and W6.48A mutants remained totally in the Rg state whatever the receptor density (Fig. 2A). As expected, the inverse agonist RO 116-1148 had no effect on the basal activity in both W6.48A (Joubert et al., 2002) and T3.36A mutants whereas it totally blocked the basal activity of the WT receptor (Fig. 2B). In conclusion, both the T3.36 and the W6.48 toggle switches were necessary to reach a R*basal.

Reaching the maximal R*-5-HT state does not require the W6.48 toggle switch whereas the T3.36 toggle switch is partially involved.

When measured at similar cell surface density, the maximal activity (E_{max}) of the R*-5-HT state in WT and W6.48A mutant were not different (Fig. 1B, Table 1). In the W6.48 mutant, the EC_{50} was shifted to the right by a factor of 25, despite the fact that the binding affinity of 5-HT for the W6.48A mutant receptor remained the same. Thus, the mutation did not affected 5-HT binding, weakly the coupling and not at all the maximal activity of the R*-5-HT state. In contrast, when measured at similar cell surface density, the maximal activity (E_{max}) of the R*-5-HT state, in the T3.36A mutant,

dropped by 26 % compared to that of the WT, whereas its EC_{50} shifted to the right by a factor of 24 and its binding affinity was also reduced by a factor of 18**.** We constructed a three-dimensional model of the complex between 5-HT and a β_2-AR-based model of the 5-HT_4R (see Methods). This computational model considers that agonists bind the active conformation of the 5-HT_4R, in which T3.36 is pointing towards TM7 in the active *g*+ conformation and W6.48 is pointing towards TM5 in the active *t* conformation. The conformation of F6.52 was also modeled in *t* to avoid the steric clash with W6.48 (Shi et al., 2002). T3.36 in *g*+ participates, in addition to the known aspartic acid D3.32 in TM3, in the binding of the protonated amine of serotonin; similar as described for histamine binding to the H_1 receptor (Jongejan et al., 2005). The indole ring of 5-HT expands toward TMs 5 and 6, to hydrogen bond the key S5.43 and N6.55 side chains (Fig. 5A), as proposed by site-directed mutagenesis (Mialet et al., 2000), without forming a direct interaction with W6.48. This mode of binding explains the fact that T3.36A slightly influences both the binding affinity for 5-HT as well as R*-5-HT (E_{max} and EC_{50}), and that W6.48A does not modify the binding affinity nor E_{max}. Thus, the W6.48 toggle switch is not necessary to reach the R*-5-HT, while the T3.36 switch is only partially necessary. R*-5-HT is probably attained through other routes of activation involving TMs 5 and 6 (see Discussion).

The R*-benzamide state is reached following a direct interaction of benzamides with T3.36, triggering its toggle switch from the g- to the g+ conformation.

Notably, the T3.36A mutation modified the process of receptor activation in an agonist-specific dependent manner (Table 1; Fig. 3B). At similar receptor expression density, the E_{max} of the R*-BIMU8 state was weakly decreased by this mutation, from 97% to 78%; while the EC_{50} was unchanged (Fig. 3; Table 1). In contrast, activation by 2-methoxy-4-amino-5-chloro benzamides (S-zacopride, cisapride) and related aryl ketone (RS 67333) was almost eliminated (Fig. 3B; Table 1). Importantly, cell surface expression of this T3.36A mutant was similar to that of the WT (Fig. 1A and legend), and the lack of stimulation was not due to a loss of binding affinity of these ligands for the 5-HT_4R-T3.36A mutant (Table 1). Since the benzamides are partial agonists on the WT receptor, it was possible that a weaker coupling efficiency due to mutation could have a higher influence on the

E_{max} of benzamides compared to that of WT. Therefore, we studied the influence of receptor density on the stimulation of 5-HT_4R by 5-HT, S-zacopride and BIMU8 in WT and T3.36A mutant (Fig. 4). We have previously shown that, in COS-7 cells (Claeysen et al., 2000), the 5-HT_4R activation can be analysed by the two-state model proposed by Leff (Leff, 1995). In particular the E_{max} increased as the function of receptor density, but the EC_{50} remains identical. This was again observed here when the dose-activation curves were determined on WT 5-HT_4R (Fig. 4, left panels). The 5-HT and BIMU8 dose-response curves determined on the T3.36A mutant also showed an increase in E_{max} without change in EC_{50} when the receptor density increased (Figs. 4D and 4F). In contrast, the benzamide S-zacopride was totally unable to stimulate the T3.36A mutant whatever the receptor density (Fig. 4E; Table 1).

In order to propose a structural hypothesis of the small effect of the T3.36A mutation on activity of the R*-BIMU8 state and the specific elimination of the R*-benzamide state we propose a model in Figs. 5B and 5C describing the complexes between these ligands and the 5-HT_4R. In addition to other pharmacophoric elements (see legend to Fig. 5), S-zacopride and BIMU8 contain key carbonyl groups, which point towards TM3 (Fig. 5B) and towards TM6 (Fig. 5C), respectively. Thus, the carbonylic oxygen of S-zacopride forms a specific hydrogen bond with the active *g*+ rotamer of T3.36 (Fig. 5B), whereas the carbonylic oxygen of BIMU8 forms the hydrogen bond interaction with the active *t* rotamer of W6.48 (Fig. 5C). Accordingly, the T3.36A mutation almost abolished the benzamide and aryl-ketone induced 5-HT_4R stimulation (Fig. 3; Table 1). We propose that benzamides and aryl ketones stabilize a R* (R*-benzamides) by triggering the direct conformational transition of T3.36 (from the inactive *g*- to the *g*+ conformation) by forming a specific hydrogen bond with T3.36.

The R*-BIMU8 state is primarily reached following a direct interaction of benzimidazolones with W6.48, and triggering its toggle switch from the g+ to t conformation.

The computational simulation presented above suggests that BIMU8 may trigger the process of 5-HT_4R activation (stabilization of the R*-BIMU8) mainly via the conformational transition of W6.48 from the *g*+ to the *t* conformation by a specific hydrogen bond interaction. To test this hypothesis, we

analysed the ability of BIMU8 to stimulate the W6.48A mutant. To our surprise the K_D value for BIMU8 was unchanged (Table), whereas this mutation reduced the EC_{50} by 43-fold (Fig. 6B) and the E_{max} by a factor of 2, compared to 5-HT stimulation (Fig. 6A). This reduction of the BIMU8-stimulation was independent of the receptor density (Fig. 6B). The effects of T3.36A and W6.48A mutations in BIMU8 function suggest that the T3.36 toggle switch plays a minor role in the stabilization of R*-BIMU8 (E_{max} decreased from 97% to 78%); leaving the W6.48 toggle switch as the main mechanism of 5-HT_4R activation by BIMU8 (E_{max} decreased from 97% to 53%). We tried to generate the double T3.36A-W6.48A mutant receptor to fully impair the R*-BIMU8 state. Unfortunately, this double mutant receptor was poorly expressed at the cell surface and no conclusion can be drawn.

Molecular modelisation showed that in the absence of W6.48 (W6.48A mutant), the aromatic ring of BIMU8 can occupy the position of the active *t* conformation of W6.48 in the WT receptor (see Fig. 6C). This position of the aromatic ring of BIMU8 in the receptor is very favourable due to the presence of the F5.47 aromatic side chain. In this new mode of binding, the carbonylic oxygen of BIMU8 forms a hydrogen bond interaction with the active *g*+ rotamer of T3.36 (Fig. 6C). Likely, in the W6.48A mutant receptor, the new R*-BIMU8 state is stabilized by this hydrogen bond, a mechanism of triggering a R* state similar to that of R*-benzamides (compare Figs. 5B and 6C). This mode of binding explains why BIMU8 has similar binding affinity for WT and W6.48A mutant 5-HT_4R. Nevertheless, the lack of expression of this double T3.36A-W6.48A mutant receptor impedes to experimentally probe this hypothesis.

DISCUSSION

One of the most important progresses in family A GPCR molecular pharmacology has been to understand, based on biophysical, biochemical and crystallography experiments, how a multitude of chemically different agonists, which do not share a common binding mode, can trigger receptor activation. A few conserved molecular activation mechanisms implying the rearrangement of the side chains of a limited number of residues have been associated with receptor activation (Kobilka, 2007; Smit et al., 2007)**.** A key question is to determine which different rearrangements of a given GPCR lead to the different R*s. Are they different for basal constitutively active R* and agonist-induced R*s? Do chemically different agonists induce different rearrangement? Few examples indicate this could be the case. In the β_2-adrenergic receptor, salbutamol although being an agonist, does not trigger the TM6 toggle switch whereas the cathecol derivatives do (Swaminath et al., 2004).

Here, we show that the R*basal of the WT 5-HT_4 receptor is likely to be the result of a simultaneous double toggle switch. One is the conformational change of W6.48 from the inactive *g*+ (pointing towards TM7) to the active *t* (TM5) conformation, which is accompanied by the conformational transition of T3.36 from the inactive *g*- (TM6) to the active *g*+ (TM7) conformation. Both coordinated switches are necessary to go from the silent Rg to the R*basal. Indeed, mutation of either W6.48 or T3.36 to alanine kept the WT 5-HT_4 receptor to the Rg state whatever the receptor density. This Rg state was, of course, insensitive to inverse agonists. When the receptor is under the Rg state, the levels of cAMP accumulation were close to those observed in the absence of receptors (the mock-transfected cells). The Rg state is not often described in GPCR pharmacology (Joubert et al., 2002). The Rg state of rhodopsin is stabilized by the full inverse agonist *cis*-retinal, the structure of which is distinct from the ligand-free opsin state R (Lin and Sakmar, 1996; Park et al., 2008).

We have also shown that T3.36, in addition to modulate the Rg to R*basal, plays a minor role in the stabilization of R*-5-HT and R*-BIMU8 and is fully required in the stabilization of the R*-benzamides (S-zacopride, cisapride and RS 67333). Benzamides were completely inactive on the T3.36A mutant, whatever the receptor density, excluding a simple reduction in the coupling efficiency affecting preferentially the response to partial agonists such as benzamides. Thus, as a hypothesis, we

can conclude that S-zacopride, cisapride, and RS 67333 trigger 5-HT_4R activation via stabilization of the rotamer toggle switch of T3.36, from the inactive *g*- to the active *g*+ conformation. Here, we show for the first time that the 3.36 position is directly implicated in agonist-induced activation and is responsible for the stabilization of an active state.

The 5-HT_4R is also activated by benzimidazolone ligands such as BIMU8. We propose that the R*-BIMU8 state is primarily reached following a direct interaction between the carbonylic oxygen of benzimidazolones and W6.48, triggering its toggle switch from the inactive *g*+ to the active *t* conformation. A similar mode of interaction between the W6.48 residue and the CSP-2503 agonist has been proposed during activation of the 5-HT_{1A} receptors (Lopez-Rodriguez et al., 2005).

It was surprising that the W6.48A as well as the T3.36A mutant were fully activated by 5-HT. This clearly indicates that the conformational mechanisms occurring from Rg to R*basal are different from those occurring from Rg to R*-5-HT. A two state model was not sufficient to explain those results. The 5-HT_4Rs as well as rhodopsin are, at least, in equilibrium between three states, i.e. the Rg, the R*basal and the R*-5-HT states. The R*-5-HT state can be reached either from the Rg or from the R*basal state. Thus, the relative stimulation by 5-HT was higher in cells expressing the receptor under the Rg state (W6.48A and T3.36A mutants) than under the R*basal state (WT receptors) (Fig. 1). A similar observation can be done considering the WT and the T3.36A mutant and the stimulation by BIMU8. The relative stimulation by BIMU8 was higher in cells expressing the T3.36A mutant (under the Rg state) than the WT receptors (under the R*basal state) (Fig. 3).

To date, there is not a clear idea as to the rearrangements occurring upon 5-HT stimulation. However, it has been shown for the β_2-adrenergic receptor, using fluorescence spectroscopy to monitor agonist-induced conformational changes, that relocation of the extracellular side of TM5 is necessary to facilitate binding of the catechol hydroxyls to the Ser residues at positions 5.42 and 5.46 (Swaminath et al., 2004). In addition, TM6 performs an inward movement of the extracellular part toward TM3 (the global toggle switch of Schwartz et al.) that is stabilized by the interaction with agonists (Schwartz et al., 2006). By homology with these proposals, we suggest that 5-HT would stabilize R*-5-HT by the interaction between the 5-OH and NH moieties with the S5.43 and N6.55 side chains, respectively, triggering the proposed movements of TMs 5 and 6.

The mechanisms by which binding of these chemical signals at the extracellular domain of the receptor trigger a set of conformational rearrangements of the TM segments near the G-protein binding domain are not fully understood. Nevertheless, comparison of the structure of inactive rhodopsin (Li et al., 2004) with the crystal structure of the ligand-free opsin (Park et al., 2008) has provided additional insights into these processes. Specifically, we propose that the T3.36/W6.48 rotamer toggle switch disrupts a conserved hydrogen bond network linking W6.48 and D2.50 (Li et al., 2004; Pardo et al., 2007; Rosenbaum et al., 2007), triggering the conformational transition of N7.49 towards D2.50 (Urizar et al., 2005), and ultimately leading to the extended conformation, pointing towards the protein core, of R3.50 (Park et al., 2008). On the other hand, the agonist-induced inward movement of the extracellular part of TM6 toward TM3 (Schwartz et al., 2006) might cause the intracellular movement of TM6 toward TM5, facilitating the observed ionic interaction between E6.30 and K5.66 (Park et al., 2008). Finally, the relocation of the extracellular side of TM5 to facilitate binding of biogenic amine agonists (Swaminath et al., 2004) induces the intracellular movement of TM5, enabling the interaction of Y5.58 with the extended conformation of R3.50 (Park et al., 2008).

We have previously established, using circular dichroism difference spectra of purified 5-HT$_4$R, that free (or neutral antagonist-occupied), agonist-occupied (partial or full agonist) and silent (inverse-agonist-occupied) receptors involved different arrangements of the e2 loop (Baneres et al., 2005). Here, in a cellular context, we provide arguments in favour of different conformational arrangements during stabilization of different 5-HT$_4$ R*s: the R*basal, the R*-5-HT, the R*-benzamides and the R*-BIMU8.

Acknowledgements

Binding experiments, cAMP measurement, and ELISA were carried out using facilities of the Pharmacological Screening platform of the Institut de Génomique Fonctionnelle. We are grateful to Angela Turner Madeuf for help in language revision and to Elisabeth Cassier for technical assistance.

REFERENCES

Alves ID, Salamon Z, Varga E, Yamamura HI, Tollin G and Hruby VJ (2003) Direct observation of G-protein binding to the human delta-opioid receptor using plasmon-waveguide resonance spectroscopy. *J Biol Chem* **278**(49):48890-48897.

Ansanay H, Sebben M, Bockaert J and Dumuis A (1996) Pharmacological comparison between [^{3}H]-GR113808 binding sites and functional 5-HT_4 receptors in neurons. *Eur J Pharmacol* **298**:165-174.

Ballesteros J and Weinstein H (1995) Integrated methods for the construction of three dimentional models and computational probing of structure-function relations in G protein coupled receptors. *Methods in Neurosciences* **25**:366-428.

Ballesteros JA, Deupi X, Olivella M, Haaksma EE and Pardo L (2000) Serine and threonine residues bend alpha-helices in the chi(1) = g(-) conformation. *Biophys J* **79**(5):2754-2760.

Baneres JL, Mesnier D, Martin A, Joubert L, Dumuis A and Bockaert J (2005) Molecular characterization of a purified 5-HT4 receptor: a structural basis for drug efficacy. *J Biol Chem* **280**(21):20253-20260.

Barthet G, Gaven F, Framery B, Shinjo K, Nakamura T, Claeysen S, Bockaert J and Dumuis A (2005) Uncoupling and endocytosis of 5-hydroxytryptamine 4 receptors. Distinct molecular events with different GRK2 requirements. *J Biol Chem* **280**(30):27924-27934.

Bond RA, Leff P, Johnson TD, Milano CA, Rockman HA, McMinn TR, Apparsundaram S, Hyek MF, Kenakin TP, Allen LF and et al. (1995) Physiological effects of inverse agonists in transgenic mice with myocardial overexpression of the beta 2-adrenoceptor. *Nature* **374**(6519):272-276.

Case D, Darden T, Cheatham T, Simmerling C and Wang J (2006) AMBER 9, University of California, San Francisco.

Cherezov V, Rosenbaum DM, Hanson MA, Rasmussen SG, Thian FS, Kobilka TS, Choi HJ, Kuhn P, Weis WI, Kobilka BK and Stevens RC (2007) High-resolution crystal structure of an engineered human beta2-adrenergic G protein-coupled receptor. *Science* **318**(5854):1258-1265.

Claeysen S, Joubert L, Sebben M, Bockaert J and Dumuis A (2003) A Single Mutation in the 5-HT4 Receptor (5-HT4-R D100(3.32)A) Generates a Gs-coupled Receptor Activated Exclusively by Synthetic Ligands (RASSL). *J Biol Chem* **278**(2):699-702.

Claeysen S, Sebben M, Becamel C, Bockaert J and Dumuis A (1999) Novel brain-specific 5-HT4 receptor splice variants show marked constitutive activity: role of the C-terminal intracellular domain. *Mol Pharmacol* **55**(5):910-920.

Claeysen S, Sebben M, Becamel C, Eglen RM, Clark RD, Bockaert J and Dumuis A (2000) Pharmacological properties of 5-Hydroxytryptamine(4) receptor antagonists on constitutively active wild-type and mutated receptors. *Mol Pharmacol* **58**(1):136-144.

Duan Y, Wu C, Chowdhury S, Lee MC, Xiong G, Zhang W, Yang R, Cieplak P, Luo R, Lee T, Caldwell J, Wang J and Kollman P (2003) A point-charge force field for molecular mechanics simulations of proteins based on condensed-phase quantum mechanical calculations. *J Comput Chem* **24**(16):1999-2012.

Ghanouni P, Gryczynski Z, Steenhuis JJ, Lee TW, Farrens DL, Lakowicz JR and Kobilka BK (2001) Functionally different agonists induce distinct conformations in the G protein coupling domain of the beta 2 adrenergic receptor. *J Biol Chem* **276**(27):24433-24436.

Jongejan A, Bruysters M, Ballesteros JA, Haaksma E, Bakker RA, Pardo L and Leurs R (2005) Linking agonist binding to histamine H1 receptor activation. *Nat Chem Biol* **1**(2):98-103.

Joubert L, Claeysen S, Sebben M, Bessis AS, Clark RD, Martin RS, Bockaert J and Dumuis A (2002) A 5-HT4 receptor transmembrane network implicated in the activity of inverse agonists but not agonists. *J Biol Chem* **277**(28):25502-25511.

Kobilka BK (2007) G protein coupled receptor structure and activation. *Biochim Biophys Acta* **1768**(4):794-807.

Leff P (1995) The two-state model of receptor activation. *Trends Pharmacol Sci* **16**(3):89-97.

Li J, Edwards PC, Burghammer M, Villa C and Schertler GF (2004) Structure of bovine rhodopsin in a trigonal crystal form. *J Mol Biol* **343**(5):1409-1438.

Lin SW and Sakmar TP (1996) Specific tryptophan UV-absorbance changes are probes of the transition of rhodopsin to its active state. *Biochemistry* **35**(34):11149-11159.

Lopez-Rodriguez ML, Morcillo MJ, Fernandez E, Benhamu B, Tejada I, Ayala D, Viso A, Campillo M, Pardo L, Delgado M, Manzanares J and Fuentes JA (2005) Synthesis and structure-activity relationships of a new model of arylpiperazines. 8. Computational simulation of ligand-receptor interaction of 5-HT(1A)R agonists with selectivity over alpha1-adrenoceptors. *J Med Chem* **48**(7):2548-2558.

McAllister SD, Hurst DP, Barnett-Norris J, Lynch D, Reggio PH and Abood ME (2004) Structural mimicry in class A G protein-coupled receptor rotamer toggle switches: the importance of the F3.36(201)/W6.48(357) interaction in cannabinoid CB1 receptor activation. *J Biol Chem* **279**(46):48024-48037.

McGregor MJ, Islam SA and Sternberg MJ (1987) Analysis of the relationship between side-chain conformation and secondary structure in globular proteins. *J Mol Biol* **198**(2):295-310.

Mialet J, Dahmoune Y, Lezoualc'h F, Berque-Bestel I, Eftekhari P, Hoebeke J, Sicsic S, Langlois M and Fischmeister R (2000) Exploration of the ligand binding site of the human 5-HT(4) receptor by site-directed mutagenesis and molecular modeling. *Br J Pharmacol* **130**(3):527-538.

Okada T, Ernst OP, Palczewski K and Hofmann KP (2001) Activation of rhodopsin: new insights from structural and biochemical studies. *Trends Biochem Sci* **26**(5):318-324.

Palczewski K, Kumasaka T, Hori T, Behnke CA, Motoshima H, Fox BA, Le Trong I, Teller DC, Okada T, Stenkamp RE, Yamamoto M and Miyano M (2000) Crystal structure of rhodopsin: A G protein-coupled receptor. *Science* **289**(5480):739-745.

Pardo L, Deupi X, Dolker N, Lopez-Rodriguez ML and Campillo M (2007) The role of internal water molecules in the structure and function of the rhodopsin family of G protein-coupled receptors. *Chembiochem* **8**(1):19-24.

Park JH, Scheerer P, Hofmann KP, Choe HW and Ernst OP (2008) Crystal structure of the ligand-free G-protein-coupled receptor opsin. *Nature* **454**(7201):183-187.

Rosenbaum DM, Cherezov V, Hanson MA, Rasmussen SG, Thian FS, Kobilka TS, Choi HJ, Yao XJ, Weis WI, Stevens RC and Kobilka BK (2007) GPCR engineering yields high-resolution structural insights into beta2-adrenergic receptor function. *Science* **318**(5854):1266-1273.

Ruprecht JJ, Mielke T, Vogel R, Villa C and Schertler GF (2004) Electron crystallography reveals the structure of metarhodopsin I. *Embo J* **23**(18):3609-3620.

Samama P, Cotecchia S, Costa T and Lefkowitz RJ (1993) A mutation-induced activated state of the b_2-adrenergic receptor. Extending the ternary complex model. *J Biol Chem* **268**:4625-4635.

Schertler GF (2005) Structure of rhodopsin and the metarhodopsin I photointermediate. *Curr Opin Struct Biol* **15**(4):408-415.

Schwartz TW, Frimurer TM, Holst B, Rosenkilde MM and Elling CE (2006) Molecular mechanism of 7TM receptor activation--a global toggle switch model. *Annu Rev Pharmacol Toxicol* **46**:481-519.

Shi L and Javitch JA (2002) The binding site of aminergic G protein-coupled receptors: the transmembrane segments and second extracellular loop. *Annu Rev Pharmacol Toxicol* **42**:437-467.

Shi L, Liapakis G, Xu R, Guarnieri F, Ballesteros JA and Javitch JA (2002) Beta2 adrenergic receptor activation. Modulation of the proline kink in transmembrane 6 by a rotamer toggle switch. *J Biol Chem* **277**(43):40989-40996.

Smit MJ, Vischer HF, Bakker RA, Jongejan A, Timmerman H, Pardo L and Leurs R (2007) Pharmacogenomic and structural analysis of constitutive g protein-coupled receptor activity. *Annu Rev Pharmacol Toxicol* **47**:53-87.

Swaminath G, Xiang Y, Lee TW, Steenhuis J, Parnot C and Kobilka BK (2004) Sequential binding of agonists to the beta2 adrenoceptor. Kinetic evidence for intermediate conformational states. *J Biol Chem* **279**(1):686-691.

Urizar E, Claeysen S, Deupi X, Govaerts C, Costagliola S, Vassart G and Pardo L (2005) An activation switch in the rhodopsin family of G protein-coupled receptors: the thyrotropin receptor. *J Biol Chem* **280**(17):17135-17141.

Visiers I, Ballesteros JA and Weinstein H (2002) Three-dimensional representations of G protein-coupled receptor structures and mechanisms. *Methods Enzymol* **343**:329-371.

Wang J, Wolf RM, Caldwell JW, Kollman PA and Case DA (2004) Development and testing of a general amber force field. *J Comput Chem* **25**(9):1157-1174.

FOOTNOTES

a)

This work was supported by grants from Centre National de la Recherche Scientifique (CNRS); Institut National de la Santé et de la Recherche Médicale (INSERM); Ministère Français de la Recherche (ANR Blanc-2006-0087-02); Université de Montpellier; Ministerio de Educación y Ciencia (SAF2006-04966, SAF-2007-67008); and Instituto de Salud Carlos III (RD07/0067/0008).

b)

Joël Bockaert

Institut de Génomique Fonctionnelle

141 Rue de la Cardonille

34094 Montpellier Cedex 5

France,

Tel: +33 467 14 29 30

Fax: +33 467 54 24 32

E-mail: joel.bockaert@igf.cnrs.fr

[1] L.P.P. and J.S. equally contributed to this work.

LEGENDS FOR FIGURES

Figure 1. Constitutive activity of the WT 5-HT$_4$R is largely dependent on T3.36.

(A) Native and mutant receptors (5-HT$_4$R-T3.36A/C/S,-W6.48A) were transiently expressed in COS-7 cells. Expression receptor levels at the plasma membrane relative to the expression of the WT were determined by ELISA assay. The relative expression levels, indicated above the graph, expressed in fmol/mg of protein, were for WT (6160 ± 1860), T3.36A (5390 ± 1010), T3.36C (4520 ± 1300), T3.36S (5300 ± 750) and W6.48 (5810 ± 1230).

(B) Basal level and maximum 5-HT (10^{-5} M) stimulation of cAMP formation were measured after 10 min incubation. Each value was estimated as the percentage of maximum cAMP production (8.9 ± 0.7 pmol/100 000 cells) in the WT induced by 5-HT (10^{-5} M).

(C) Statistical preferences of threonine (T), serine (S), and cysteine (C) side chain rotamer distribution (*t*: *trans*, *g*+: *gauche*+ or *g*-: *gauche*-; see Methods*)* when located in a α-helical structure (adapted from Ballesteros et al. (Ballesteros et al., 2000)). Active conformations in the 5-HT$_4$R are shown in bold and asterisked.

(D) 5-HT$_4$R activation consists of a concerted T3.36/W6.48 rotamer toggle switch. T3.36 undergoes a conformational transition from the inactive *g*- to the active *g*+ conformation, in conjunction with the conformational transition of W6.48 from the inactive *g*+ to the active *t* conformation.

Figure 2. Lack of basal activity and inverse agonist RO 116-1148 effect in T3.36A and W6.48A mutants.

(A) The relationship between receptor density and basal activity was measured in COS-7 cells expressing increasing density of WT, T3.36A and W6.48A. cAMP production was expressed as a percentage over basal cAMP produced in the mock-transfected cells (0.13 ± 0.03 pmol/100 00 cells).

(B) The inverse agonist activity of RO 116-1148 was tested relative to basal constitutive cAMP production in WT, T3.36A and W6.48A. The inverse agonist effect is represented as the percentage of basal cAMP formation taken as 100% (2.86 ± 0. 15 pmol/100 000 cells for 200 ng of WT 5-HT$_4$R

cDNA transfected). Each value represents the mean ± SEM determined from three independent experiments performed in triplicate.

Figure 3. Influence of T3.36 in the agonist-induced activation of the 5-HT_4R.

Intracellular cAMP levels were measured in COS-7 cells transiently expressing 6160 and 5390 fmol/mg protein of WT 5-HT_4R **(A)** and T3.36A mutant receptor **(B)**, respectively, in the presence of agonists belonging either to the indol (5-HT), or benzamide (S-zacopride, cisapride), or aryl ketone (RS 67333) or benzimidazolone (BIMU8) classes. Results are expressed as a percentage of the maximum cAMP production (8.9 ± 0.7 pmol/100 000 cells) induced by stimulating WT receptor with 5-HT (10^{-5} M). Each value represents the mean ± SEM determined from three independent experiments performed in triplicate. Structures of the drugs used in the study are presented below the graph. Oxygen of the carbonyl group that interacts either with T3.36 or with W6.48 is asterisked.

Figure 4. Effect of increasing T3.36A receptor density on agonist activation.

cAMP accumulation at different densities of WT (A-C) and T3.36A (D-F) 5-HT_4Rs, transiently expressed in COS-7 cells, was measured over 10 min-stimulation induced by 5-HT **(A, D)**, S-zacopride **(B, E)** or BIMU8 **(C, F)**. *Data are expressed as a percentage of maximal stimulation due to 5-HT in WT expressing the highest receptor density (31100 fmol/mg protein). COS-7 cells were transfected with increasing amount of DNA (50, 100, 200 and 500 ng) corresponding to 5370 ± 1830, 9510 ± 1070, 19840 ± 2300 and 31100 ± 1600 fmol/mg protein for WT and 4900 ± 880, 8950 ± 130, 17870 ± 750 and 28300 ± 3950 fmol/mg of protein for T3.36A mutant.

Figure 5. Computational models of the complexes between 5-HT_4R and BIMU8 or Zacopride.

In these models the protonated moiety of the ligands interact with D3.32; the 5-OH and NH moieties of 5-HT hydrogen bond the key S5.43 and N6.55 side chains **(A)** as proposed by site-directed mutagenesis (Mialet et al., 2000); the $–C(CH_3)_2$ and –Cl moieties of BIMU8 and S-zacopride, respectively, are located in a small hydrophobic cavity between TMs 3-5 **(B, C)**; and the $–NH_2$ group of S-zacopride hydrogen bonds S5.43 **(B)**. BIMU8 and S-zacopride form an intramolecular hydrogen

bond between the –NH amide and a carbonyl or methoxy group, respectively. BIMU8 elicits 5-HT_4R activation by forming a hydrogen bond interaction with W6.48 in the active *t* conformation **(C)**, while S-zacopride triggers activation via the interaction with T3.36 in the active *g*+ conformation **(B)**. The atoms implicated in these interactions are pointed out: oxygen of the drugs is asterisked and T3.36 or W6.48 hydrogen is labelled with a filled square.

Figure 6. Influence of W6.48 in the BIMU8-induced activation of the 5-HT_4R.

cAMP accumulation at different densities of 5-HT_4-W6.48A mutant, transiently expressed in COS-7 cells, was measured over 10 min-stimulation induced by 5-HT **(A)** or BIMU8 **(B)**. *Data are expressed as a percentage of maximal stimulation due to 5-HT in W6.48A mutant expressing the highest receptor density (6490 fmol/mg protein). COS-7 cells were transfected with increasing amount of DNA (200, 500, 1000 and 2000 ng) corresponding to 1080 ± 260, 2690 ± 280, 4080 ± 880 and 6490 ± 520 fmol/mg protein of W6.48A mutant.

(C) Computational models of the complex between BIMU8 and W6.48A mutant receptor. In the absence of W6.48, the aromatic ring of BIMU8 occupies the position of the active *t* conformation of W6.48 in the WT receptor (see Fig. 5C); and the carbonylic oxygen hydrogen bonds the active *g*+ rotamer of T3.36. The atoms implicated in this interaction are pointed out: oxygen of the drug is asterisked and T3.36 hydrogen is labelled with a filled square.

TABLE 1

Pharmacological properties of a series of 5-HT_4R ligands on WT $5HT_4$R, T3.36A and W6.48A mutant receptors.

All the data are expressed as means ± SEM of at least four separate experiments.

[a] Binding assays were performed by using [^{3}H]GR 113808 as the specific 5-HT_4R radioligand in COS-7 cells membranes expressing either WT 5-HT_4R, 5-HT_4-T3.36A or 5-HT_4-W6.48A. Non-specific binding was determined with BIMU8 (10 µM). K_D values were determined from Cheng-Prussoff equation.

[b] The agonist activity or potency (EC_{50}) was accessed as the concentration that gave 50% increase in the response to cAMP formation.

[c] The maximal activity of each drug (E_{MAX}) is expressed as percentage of the maximum 5-HT response obtained with the WT at similar receptor density.

ND: non determined.

	WT			T3.36A			W6.48A		
	K_D (M)[a]	EC_{50} (M)[b]	E_{MAX}[c]	K_D (M)[a]	EC_{50} (M)[b]	E_{MAX}[c]	K_D (M)[a]	EC_{50} (M)[b]	E_{MAX}[c]
5-HT	$7.7 \pm 1.4\ 10^{-8}$	$3.6 \pm 0.7\ 10^{-9}$	100%	$1.4 \pm 2.3\ 10^{-6}$	$8.6 \pm 3.3\ 10^{-8}$	74 ± 1%	$7.4 \pm 2.6\ 10^{-8}$	$8.9 \pm 3.2\ 10^{-8}$	100%
BIMU8	$5.3 \pm 1.2\ 10^{-8}$	$1.8 \pm 0.7\ 10^{-8}$	97 ± 4%	$2.1 \pm 0.1\ 10^{-7}$	$7.7 \pm 1.7\ 10^{-8}$	78 ± 2%	$1.1 \pm 0.7\ 10^{-7}$	$5.4 \pm 1.9\ 10^{-7}$	53 ± 3%
S-zacopride	$6.4 \pm 0.9\ 10^{-7}$	$1.1 \pm 0.2\ 10^{-7}$	77 ± 1%	$7.2 \pm 1.5\ 10^{-7}$	ND	ND			
Cisapride	$2.0 \pm 0.2\ 10^{-7}$	$4.3 \pm 3.1\ 10^{-8}$	64 ± 1%	$7.3 \pm 1.4\ 10^{-7}$	ND	ND			
RS 67333	$5.5 \pm 0.2\ 10^{-9}$	$2.6 \pm 1.5\ 10^{-9}$	70 ± 2%	$1.2 \pm 0.3\ 10^{-8}$	ND	ND			

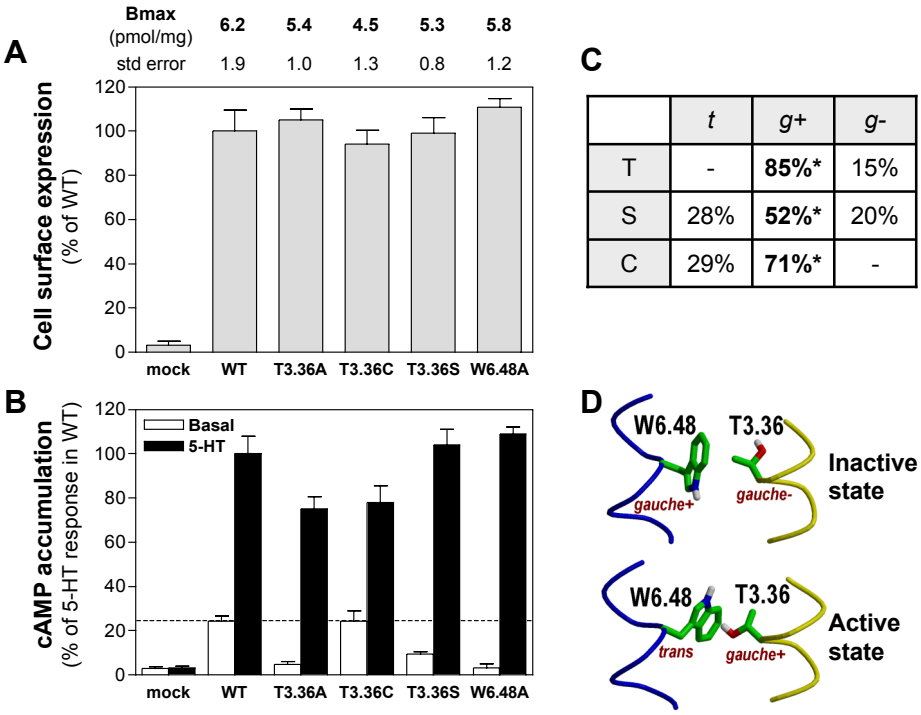
A
Bmax (pmol/mg)
6.2
5.4
4.5
5.3
5.8
std error
1.9
1.0
1.3
0.8
1.2
Cell surface expression (% of WT)
120
100
80
60
40
20
0
mock
WT
T3.36A
T3.36C
T3.36S
W6.48A
B
cAMP accumulation (% of 5-HT response in WT)
Basal
5-HT
120
100
80
60
40
20
0
mock
WT
T3.36A
T3.36C
T3.36S
W6.48A
C
t
g+
g-
T
-
85%*
15%
S
28%
52%*
20%
C
29%
71%*
-
D
W6.48
T3.36
gauche+
gauche-
Inactive state
W6.48
T3.36
trans
gauche+
Active state

Figure 1

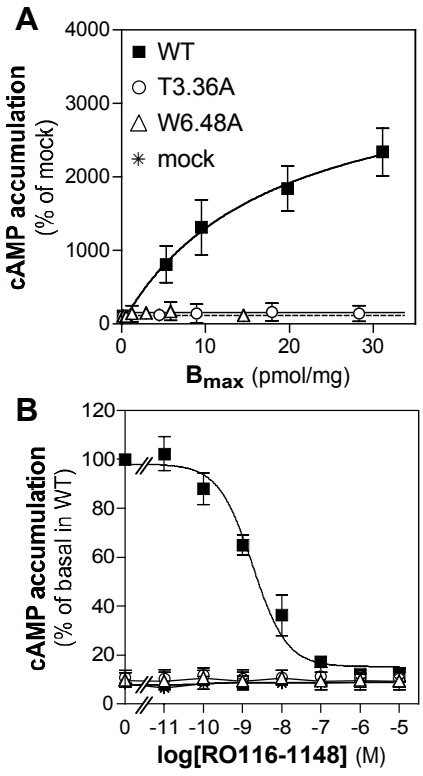
A
4000
3000
2000
1000
0
WT
T3.36A
W6.48A
mock
cAMP accumulation
(% of mock)
0
10
20
30
Bmax (pmol/mg)
B
120
100
80
60
40
20
0
cAMP accumulation
(% of basal in WT)
0
-11
-10
-9
-8
-7
-6
-5
log[RO116-1148] (M)

Figure 2

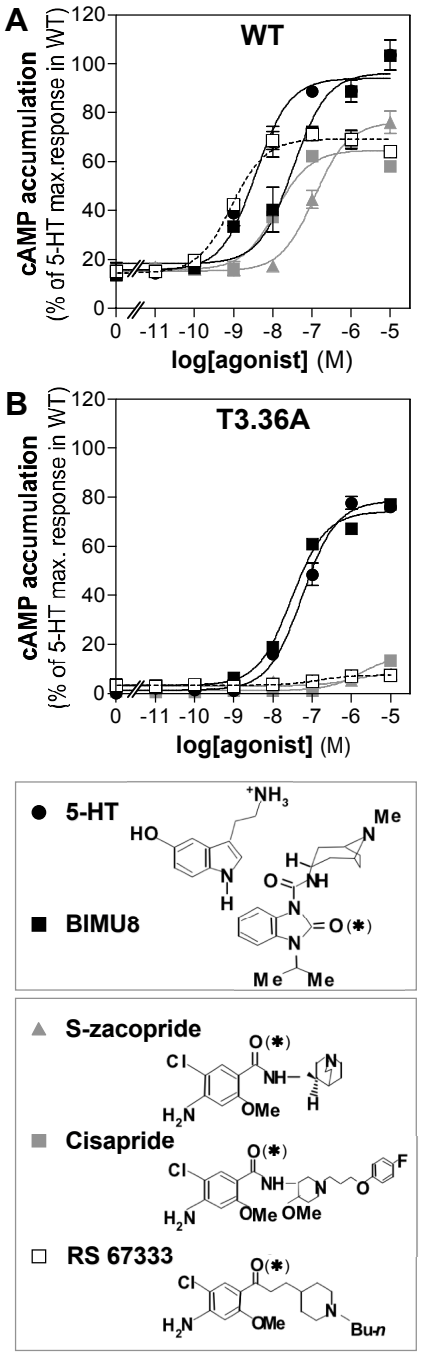
A
WT
cAMP accumulation
(% of 5-HT max.response in WT)
120
100
80
60
40
20
0
0 -11 -10 -9 -8 -7 -6 -5
log[agonist] (M)
B
T3.36A
cAMP accumulation
(% of 5-HT max. response in WT)
120
100
80
60
40
20
0
0 -11 -10 -9 -8 -7 -6 -5
log[agonist] (M)
5-HT
BIMU8
S-zacopride
Cisapride
RS 67333

Figure 3

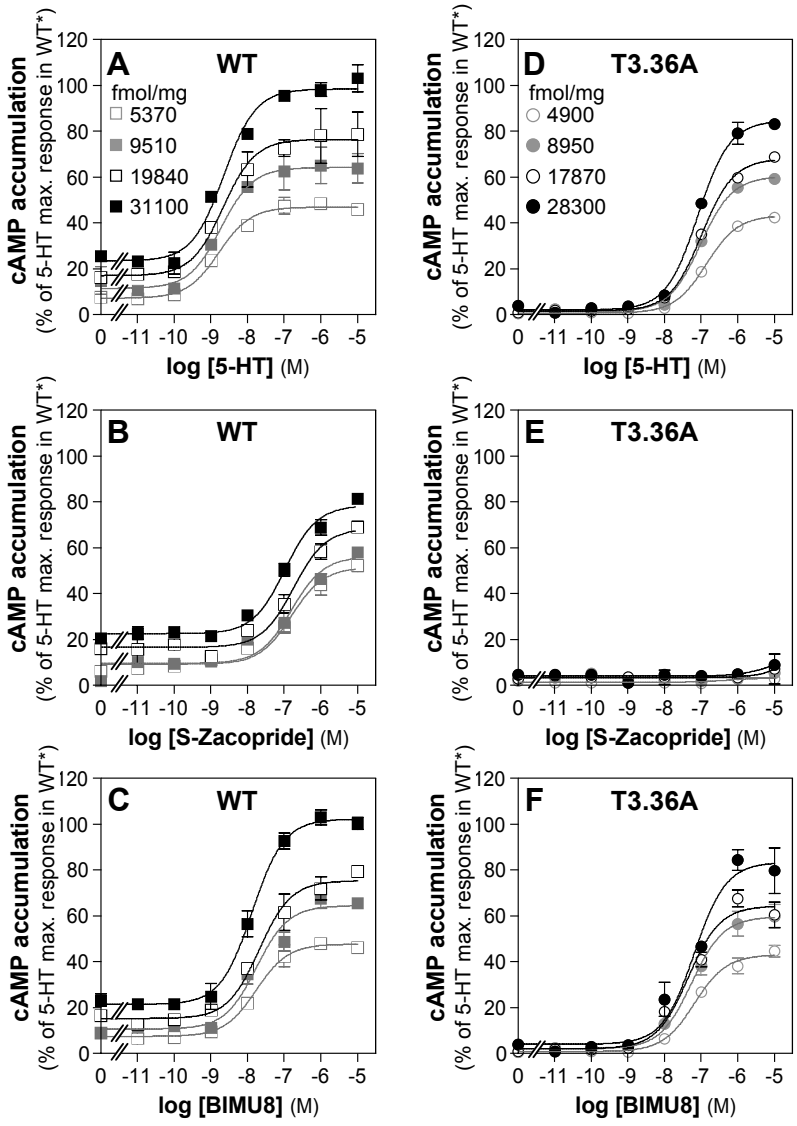
A
WT
fmol/mg
5370
9510
19840
31100
D
T3.36A
fmol/mg
4900
8950
17870
28300
B
WT
E
T3.36A
C
WT
F
T3.36A
cAMP accumulation
(% of 5-HT max. response in WT*)
log [5-HT] (M)
log [S-Zacopride] (M)
log [BIMU8] (M)

Figure 4

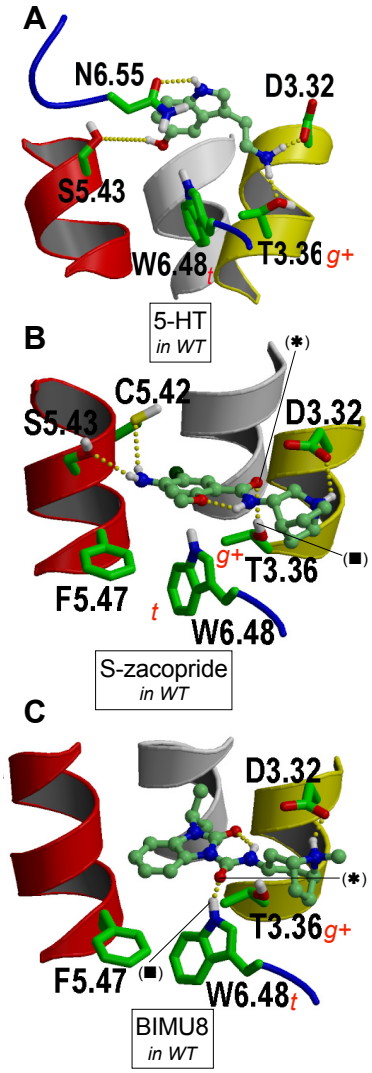
A
N6.55
D3.32
S5.43
W6.48 t
T3.36 g+
5-HT
in WT
B
C5.42
S5.43
D3.32
(*)
g+
T3.36
(■)
F5.47
t
W6.48
S-zacopride
in WT
C
D3.32
(*)
T3.36 g+
F5.47
(■)
W6.48 t
BIMU8
in WT

Figure 5

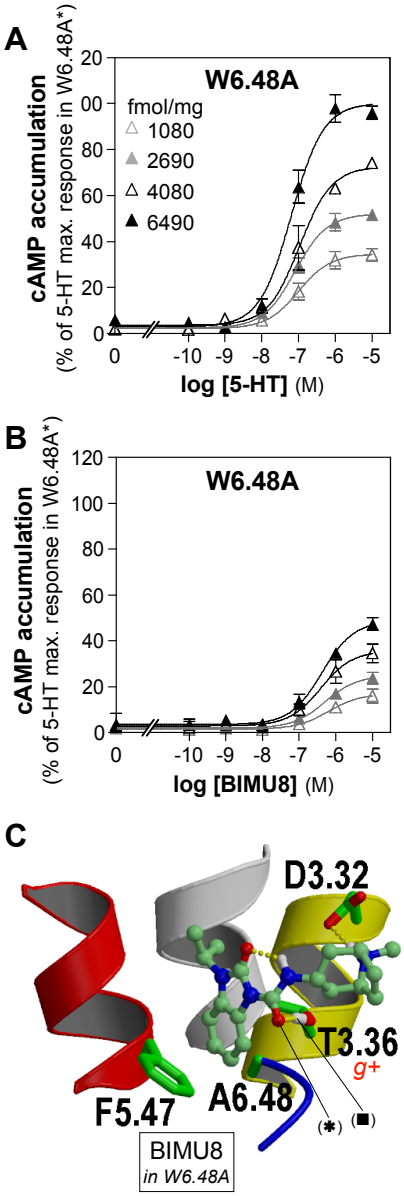
A
W6.48A
fmol/mg
1080
2690
4080
6490
cAMP accumulation
(% of 5-HT max. response in W6.48A*)
log [5-HT] (M)
B
W6.48A
cAMP accumulation
(% of 5-HT max. response in W6.48A*)
log [BIMU8] (M)
C
D3.32
T3.36
g+
F5.47
A6.48
(*)
(■)
BIMU8
in W6.48A

Figure 6